



Preparation, characterization, and application of sludge with additive scrap iron-based activated carbons

Xin Li^a, Wei-guang Li^{b,*}, Guang-zhi Wang^a, Ping Wang^a, Xu-jin Gong^a

^aSchool of Municipal and Environmental Engineering, Harbin Institute of Technology, Harbin, Heilongjiang 150090, China

^bState Key Laboratory of Urban Water Resource and Environment, Harbin Institute of Technology, Harbin, Heilongjiang 150090, China, Tel. +86 15245066316; email: lixin861221@yeah.net

Received 24 November 2013; Accepted 14 February 2014

ABSTRACT

Activated carbons were prepared using sewage sludge with additive scrap iron as precursor and ZnCl₂ as activator by pyrolysis method. By examining the effects of pyrolysis temperature, pyrolysis time, impregnation ratio, and scrap iron dosage on the adsorption performance of the sludge with additive scrap iron-based activated carbon, the optimum preparation conditions were obtained as following: pyrolysis temperature of 550°C, pyrolysis time of 50 min, impregnation ratio of 3:1, and scrap iron dosage of 0.5 wt %. The physical and chemical characteristics of the activated carbons produced from sewage sludge with and without additive scrap iron were determined and compared. The results showed that adding scrap iron into sewage sludge could enhance the pyrolysis of sludge and significantly improve the formation of mesopores in the produced activated carbon. In the adsorption experiments applying the prepared activated carbons to the treatment of azo dye wastewater, the adsorption data fitted the Langmuir model well. The adsorption performance of the activated carbon for the dye was remarkably enhanced after the addition of scrap iron, with the maximum adsorption capacity increasing from 156.25 to 243.31 mg/g.

Keywords: Sewage sludge; Scrap iron; Pyrolysis; Activated carbon; Mesopores; Dye adsorption

1. Introduction

With large-scale construction of wastewater treatment plants and improvement of wastewater treatment efficiency, sewage sludge production grows significantly. Sewage sludge is a kind of semi-solid waste with complex rheological properties. It not only

contains a large number of organic compounds but also some hazardous substances such as pathogenic micro-organisms, bacteria, and heavy metals [1,2]. Therefore, sludge must be disposed properly in case of secondary pollution [3]. The traditional methods for the sludge disposal are landfill, agricultural use, incineration, etc. However, there are some defects in these methods [4]. Sewage sludge is carbonaceous and has

*Corresponding author.

Presented at the 6th International Conference on the "Challenges in Environmental Science and Engineering" (CESE-2013), 29 October—2 November 2013, Daegu, Korea

high calorific value and high content of dry basis volatile. Accordingly, sewage sludge can be converted into activated carbon under certain conditions. Several studies have demonstrated the feasibility of this conversion [5–7].

In recent years, many researchers have been paying a growing attention to prepare activated carbon from sewage sludge with additive waste materials. It can not only improve the performance of the produced activated carbon, but also make sewage sludge and waste materials disposed simultaneously in an environmentally friendly way. Tay et al. [8] prepared activated carbons from anaerobically digested sewage sludge with additive coconut husk and found that the role of increasing the mixing ratio of coconut husk to sewage sludge was principally to increase microporosity of the final products. Wu et al. [9] used sewage sludge with additive corn cob as starting material to prepare activated carbons and found the addition of corn cob into the sludge sample could effectively improve the surface area and microporosity of the produced activated carbons. Seredych and Bandosz [10] produced a new class of reactive adsorbents obtained by pyrolyzing the mixture of sewage sludge and industrial oil sludge, which can be used for the removal of cationic and anionic dyes. The high adsorption efficiency of such adsorbents for both dyes was linked to surface chemical heterogeneity and a high volume of mesopores.

Scrap iron is a kind of solid wastes produced during the mechanic processing of metals. Unlike most organic contaminants, metal contaminants are especially problematic because they are persistent and non-biodegradable in natural environment [11]. Therefore, recovery and recycling of scrap iron are quite important to the environment and public health. The preparation of activated carbon from sewage sludge with additive scrap iron has provided a possible way to deal with such metal contaminants. To the best of our knowledge, it has not been reported previously.

One important application of activated carbon is the treatment of wastewater containing synthetic organic dyes which are extensively used in textile, paper, leather, cosmetics, pharmaceuticals, and food industries [12]. Azo dyes which have azo bonds ($-N=N-$) in their chemical structures account for over half of the commercial dyes [13]. Large quantities of industrial wastewater containing such dyes are discharged into water bodies. The dyes in the water bodies which are highly visible are the first contaminants to be recognized. In addition, most of these dyes are toxic, mutagenic and carcinogenic, and posing a serious threat to human and environmental health [14]. Adsorption is considered to be a promising technique for the removal of this kind of dyes [15,16].

In this study, the sludge with additive scrap iron-based activated carbon (SSIBAC) was prepared by pyrolysis method using zinc chloride as an activating agent. The effects of preparation condition parameters such as pyrolysis temperature, pyrolysis time, impregnation ratio (i.e. ratio of the volume of $ZnCl_2$ solution to the mass of starting material), and scrap iron dosage on the adsorption performance of SSIBAC were investigated to seek an optimum preparation condition. To evaluate the effect of scrap iron addition, activated carbons prepared from the sludge with and without additive scrap iron were both characterized by various techniques. Then the produced activated carbons were applied to treat azo dye wastewater. An anionic azo dye, Acid Orange 51, was selected for the adsorption tests.

2. Experimental methods

2.1. Preparation of the activated carbons

The raw materials for activated carbon preparation were aerobically digested and dewatered sewage sludge from an urban wastewater treatment plant located in Harbin, China. Ultimate and proximate analyses of the sewage sludge are shown in Table 1. The scrap iron used in this study originated from a metal processing plant in Harbin, China. The scrap iron was washed several times with warm water to assure the impurities were removed completely and dried in a draught drying cabinet at 105°C. Although no chemical or physical characterization was conducted, the presence of oxides on the surface of scrap iron was visible. It has been previously reported that the oxides generated on the surface of scrap iron are composed of an inner layer of ferrous oxide coated with an outer layer of ferric oxide [17,18].

The pyrolysis temperature, pyrolysis time, impregnation ratio, and scrap iron dosage are considered as key parameters for preparing the SSIBAC. Detailed preparation procedure is as follows. The sludge sample was dried to constant weight at 105°C, and

Table 1
Ultimate and proximate analyses of the sewage sludge

Ultimate analysis (wt %)					Proximate analysis (wt %)			
C_{ad}	H_{ad}	N_{ad}	S_{ad}	O_{ad}^b	M_{ar}	V_{ad}	A_{ad}	FC_{ad}
28.40	3.54	2.68	1.17	16.11	79.65	41.53	48.10	10.37

Note: M, moisture content; V, volatile matters; A, ash; FC, fixed carbon; ad, on dry basis; ar, on as-received basis; b, determined by difference.

then crushed and sieved into a uniform particle size of 0.15 mm approximately. Measured amounts of fine scrap iron powder from 0 to 2 wt % were thoroughly added to each 10 g sludge sample. Following that, the samples were impregnated in 4 M ZnCl₂ solution with a given impregnation ratio at 45°C for 24 h. After the supernatant liquid was removed, the samples were dried once again at 105°C for 24 h. The resulting chemically activated samples were subsequently pyrolyzed in a tubular furnace to the pyrolysis temperature with a heating rate of 15°C/min. The samples were held for a variable pyrolysis time at the pyrolysis temperature. Nitrogen was used as purge gas with a flow rate of 300 mL/min. When the pyrolysis process was completed, the samples were cooled to room temperature in the inert atmosphere. The pyrolysis products were washed with 3 M HCl to eliminate the remains of the activating agent and the fraction of soluble ash, and then washed with distilled water to remove excess acid until the pH of the rinse water was 5–6. The products were dried, crushed, sieved, and collected for further testing and application.

To understand the effect of additive scrap iron on the characteristics of the produced activated carbon, the sludge-based activated carbon (SBAC), which is without additive scrap iron, was also prepared. The preparation method was consistent with that described above and the preparation conditions were the optimum pyrolysis temperature, pyrolysis time, and impregnation ratio determined in the above experiments.

2.2. Characterization of the activated carbons

The iodine and methylene blue values of the activated carbons were determined according to the ASTM standard method (ASTM D4607-94) [19] and the Standard testing method of Methylene Blue Number of Activated Carbon (JIS K 1470–1991) [20], respectively.

Physical characteristics of the activated carbons including specific surface area (S_{BET}), total pore volume (V_t), micropore volume (V_{micro}), mesopore volume (V_{meso}), and average pore diameter (D_p) were obtained by nitrogen adsorption at 77 K with a Micromeritics model ASAP2020 sorptometer. S_{BET} was calculated by the Brunauer–Emmet–Teller method. V_{micro} and V_{meso} were calculated by the t -plot method. V_t and D_p were determined by the Barrette–Joyner–Halenda (BJH) method. The mesopore and micropore size distributions were determined according to the BJH and the Horvath–Kawazoe method, respectively.

The surface functional groups of the activated carbons were analyzed with Fourier transform infrared spectroscopy (FTIR) (Spectrum One B, USA). Each

sample was mixed with KBr before analysis. The scanning range of IR was 4,000–400 cm⁻¹, in terms of wavenumber. The resolution and the number of scans were set at 4 cm⁻¹ and 10 times, respectively.

2.3. Equilibrium adsorption tests

Acid Orange 51 (AO51) was purchased from XINHUA textile company in Harbin, China and used without further purification. The properties of AO51 are summarized in Table 2 and its chemical structure is shown in Fig. 1. Dye molecular size, including width, length, and depth, was measured by Molecular Mechanics 2 under the CambridgeSoft Chem3D Ultra 8.0 interface [21].

The adsorption experiments were carried out in a series of stoppered conical flasks (250 mL) containing doses of the activated carbons ranging from 0.2 g/L to 0.8 g/L and 100 mL AO51 solutions at an initial concentration of 100 mg/L in an isothermal (25°C) water bath shaker operated at 120 rpm. For each set of experiments, a blank test (without activated carbons) was always carried out. After shaking for the equilibrium time determined in previous tests, the flasks were removed and the suspension was filtrated through a Whatman 2 V filter paper. The first part of the filtrate was discarded to eliminate the influences of any adsorption on the filter paper. The dye concentration was analyzed using a UV–vis spectrophotometer (UV759CRT, Shang Hai) by measuring the absorbance at λ_{max} of 446 nm. Calibration curve was established prior to the analysis. Dilutions were conducted where necessary to make the absorbance of analyte solutions within the calibration range. The amount of dye adsorption at equilibrium, q_e (mg/g) was calculated. All the experiments were repeated twice and the average values of the results are presented in this work. For comparison, experiments were simultaneously done using a commercial wooden activated carbon with carbon content of 71.3% and S_{BET} of 630.79 m²/g.

Table 2
Properties of Acid Orange 51

Property	Acid Orange 51
Molecular formula	C ₃₆ H ₂₆ N ₆ Na ₂ O ₁₁ S ₃
Molecular weight (g/mol)	860.8
Width (nm)	0.92
Length (nm)	2.96
Depth (nm)	0.9
λ_{max}^a (nm)	446

^aMaximum adsorption wavelength.

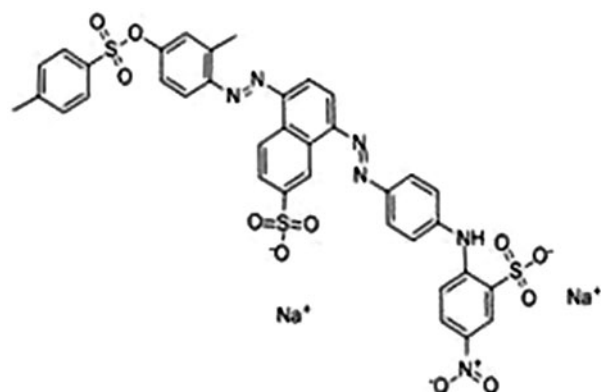


Fig. 1. The chemical structure of Acid Orange 51.

3. Results and discussion

3.1. Optimization of the preparation condition

To optimize the preparation condition, the effects of important variables such as pyrolysis temperature, pyrolysis time, impregnation ratio, and scrap iron dosage on the adsorption performance of SSIBAC were investigated. Generally, the iodine and methylene blue adsorption values are adopted to characterize the adsorption capability of activated carbon. The iodine value reflects the amount of micropores and the methylene blue value reflects the amount of mesopores of activated carbon [22].

The effect of pyrolysis temperature on the iodine value and methylene blue value of SSIBAC is shown in Fig. 2. It can be seen that below 550°C, the iodine value and methylene blue value increase with increase in the pyrolysis temperature. When the temperature exceeds

550°C, the iodine value and methylene blue value begin to take on a decrease tendency with temperature increasing. This phenomenon can be explained by two reasons. First, as the temperature increases above 550°C, the evaporation rate of ZnCl₂ keeps rising, subsequently making the amount of ZnCl₂ remaining in the sample decrease. The mechanism of pore formation during pyrolysis is that the organic matters in the starting material are converted into volatiles and polymerized carbon through polycondensation and cross-linking reactions, and pores are formed when the volatiles pass through carbon layers. The activating agent influences pyrolysis in term of promoting polycondensation and cross-linking reactions. A decrease in the amount of ZnCl₂ results in polycondensation and cross-linking reactions proceeding slowly, and hence porosity development decreases. Second, high pyrolysis temperature enhances carbon loss, thereby increasing the ash content. That ash content confines the porosity development occurring within organic matters and behaves only as an inert component which does not contribute to the porosity [23]. Therefore, 550°C is selected as the optimum pyrolysis temperature.

Fig. 3 shows the effect of pyrolysis time on the iodine value and methylene blue value of SSIBAC. As seen from figure, the iodine value and methylene blue value firstly increase and then decrease with the extension of pyrolysis time. As mentioned above, the volatilization of organic matters during pyrolysis improves the material's porosity. When pyrolysis time is shorter than 50 min, the reaction of organic matters is not sufficient, thus generating fewer volatiles, which leads to the underdevelopment of porosity. When pyrolysis time is longer than 50 min, the adsorption

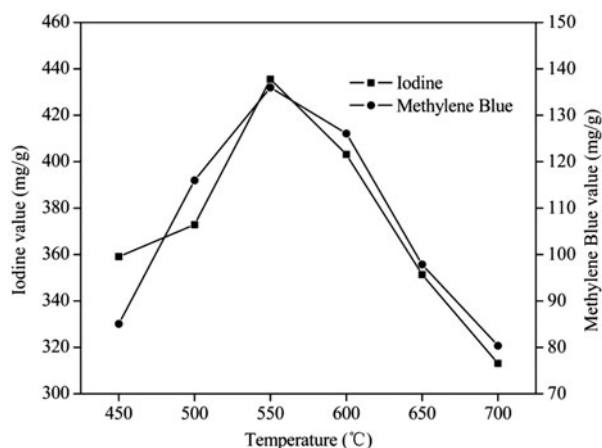


Fig. 2. Effect of pyrolysis temperature on the iodine value and methylene blue value of SSIBAC. Pyrolysis time: 50 min; impregnation ratio: 3:1; scrap iron dosage: 0.5 wt %.

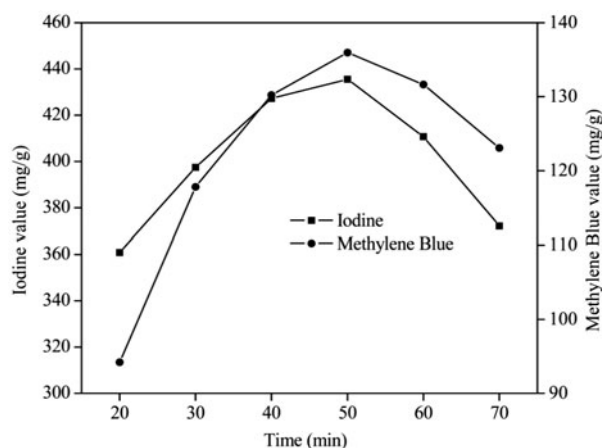


Fig. 3. Effect of pyrolysis time on the iodine value and methylene blue value of SSIBAC. Pyrolysis temperature: 550°C; impregnation ratio: 3:1; scrap iron dosage: 0.5 wt %.

capability decreases, probably due to a sintering effect occurring in the adjacent pores. Accordingly, the optimum pyrolysis time is 50 min.

The effect of impregnation ratio on the iodine value and methylene blue value of SSIBAC is depicted in Fig. 4. As can be seen from Fig. 4, the optimum impregnation ratio is 3. When the impregnation ratio is lower than 3, the relatively lack of activating agent cannot activate the organic matters in the sample sufficiently, thus the porosity is not well-developed. Increasing the impregnation ratio over the optimum value negatively affects the adsorption capacity of SSIBAC, which is attributed to the blockage of some

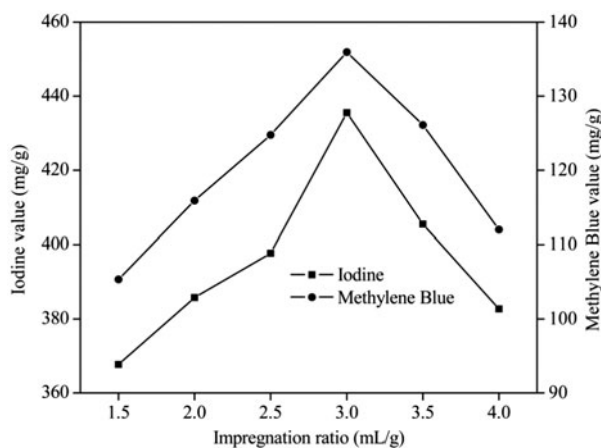


Fig. 4. Effect of impregnation ratio on the iodine value and methylene blue value of SSIBAC. Pyrolysis temperature: 550°C; pyrolysis time: 50 min; scrap iron dosage: 0.5 wt %.

pores, caused by the remaining $ZnCl_2$ which is not completely removed by post-pyrolysis washing.

The effect of scrap iron dosage on the iodine value and methylene blue value of SSIBAC is presented in Fig. 5. The scrap iron dosage ranges from 0.2 to 2 wt %. For the activated carbons prepared with additive scrap iron, an increase in both the iodine value and methylene blue value is observed and the largest adsorption values are both obtained at the scrap iron dosage of 0.5 wt %. Once the dosage exceeds 0.5 wt %, the adsorption capacity of SSIBAC decreases; suggesting the scrap iron functions well only within a certain range of dosage. It can be explained by that there are a certain amount of active sites in the inner structure that scrap iron can access to, thus the maximized effect occurs when the active sites available in the carbon matrix are fully occupied by the scrap iron particles [24].

As investigated above, the optimum conditions for the preparation of SSIBAC are as following: pyrolysis temperature of 550°C; pyrolysis time of 50 min; impregnation ratio of 3:1; scrap iron dosage of 0.5 wt %.

3.2. Characterization of the activated carbons

3.2.1. Physical characteristics of the activated carbons

The porous structure characteristics of activated carbons are determined from their nitrogen adsorption isotherms. The nitrogen adsorption–desorption isotherms of SBAC and SSIBAC are presented in Fig. 6. As illustrated in Fig. 6, compared to the SBAC, the

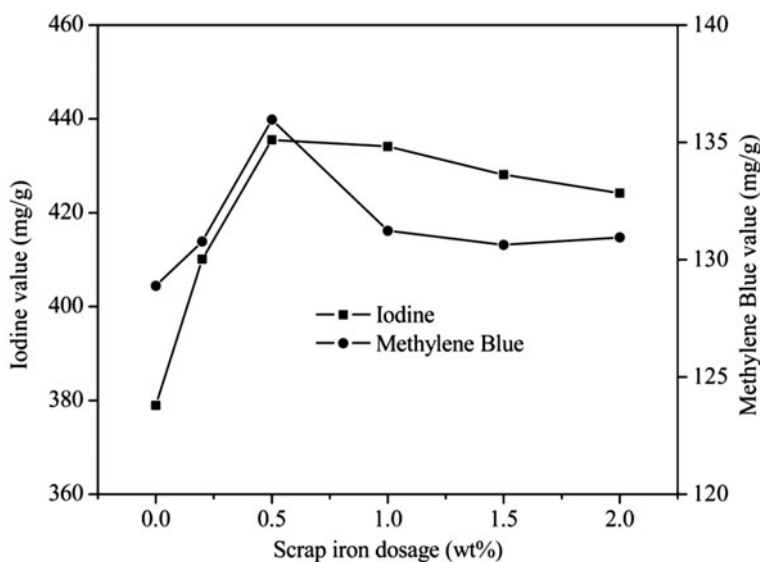


Fig. 5. Effect of scrap iron dosage on the iodine value and methylene blue value of SSIBAC. Pyrolysis temperature: 550°C; pyrolysis time: 50 min; impregnation ratio: 3:1.

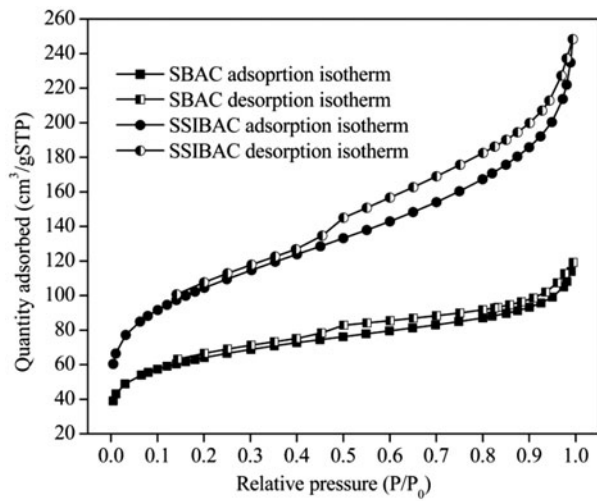


Fig. 6. Nitrogen adsorption–desorption isotherms of SBAC and SSIBAC.

nitrogen uptake of SSIBAC significantly increases. Furthermore, for both activated carbons, the rapidly increasing nitrogen adsorption volume and the almost completely overlapped adsorption/desorption isotherms at low relative pressures indicate the existence of micropores. With relative pressures increasing, hysteresis exists, suggesting the existence of mesopores in SBAC and SSIBAC.

The porous structure parameters obtained from nitrogen isotherms are listed in Table 3, including specific surface area, porous volumes, and average pore diameter. As reported in Table 3, the addition of scrap iron into sewage sludge results in an increase in both specific surface area and total pore volume. The specific surface area of SSIBAC is approximately 65% larger than that of SBAC. The total pore volume is increased from 0.162 to 0.331 cm³/g, which is primarily attributed to the generation of more mesopores. This can be seen from the improvement of mesoporosity, defined as the ratio of mesopore volume to total pore volume, which is increased from 78 to 89% after the addition of scrap iron. Furthermore, the larger average pore diameter of SSIBAC also indicates that more mesopores than micropores are produced due to the additive scrap iron.

Fig. 7 shows the pore size distributions of SBAC and SSIBAC. For SBAC and SSIBAC, the mesopore characteristics are dominant. The additive scrap iron evidently enhances the production of mesopores. However, the improvement in the formation of micropores is insignificant.

The mechanism of promoting the formation of mesopores by metal compounds is not clear. Marsh and Tomita [25,26] speculated that the activation was carried out in the immediate vicinity of the metal particles, resulting in the formation of mesopores by pitting holes into the carbon matrix. The scrap iron consists of zero-valent iron, ferric oxide, ferrous oxide, and other iron complexes, which may promote the formation of mesopores during pyrolysis. The similar function of other transition metals and their compounds has been reported in the literature [27–29].

3.2.2. Chemical characteristics of the activated carbons

Normally, FTIR is adopted to analyze the surface functional groups of activated carbons. The FTIR spectra of SBAC and SSIBAC are shown in Fig. 8. The broad band at 3,430 cm⁻¹ could be assigned to hydroxyl group (–OH) and/or amine group (–NH₂). The band at around 1,640 cm⁻¹ is assigned to carbonyl group (C=O), which is possibly in enolic form. The strong band observed at 1,050 cm⁻¹ is assigned to C–O structures [30]. Moreover, some adsorption bands occurring in the range of 700–900 cm⁻¹ are assigned to aromatic hydrogen [31]. As shown in Fig. 8, the difference between the FTIR spectra of SBAC and SSIBAC is insignificant, indicating that these two activated carbons have similar surface chemical characteristics. Nevertheless, some changes can be observed through careful distinction: the –NH₂, –OH, and C=O functionalities decrease slightly after the addition of scrap iron, indicating that adding scrap iron can enhance the pyrolysis of sludge.

3.3. Adsorption performance of the activated carbons for Acid Orange 51

To determine the adsorption performance of the activated carbons for AO51, adsorption experiments

Table 3
Characteristics of the porous structure of SBAC and SSIBAC

Activated carbon	S_{BET} (m ² /g)	V_t (cm ³ /g)	V_{micro} (cm ³ /g)	V_{meso} (cm ³ /g)	V_{meso}/V_t	D_p (nm)
SBAC	225.09	0.162	0.036	0.126	0.78	2.89
SSIBAC	370.96	0.331	0.038	0.293	0.89	3.56

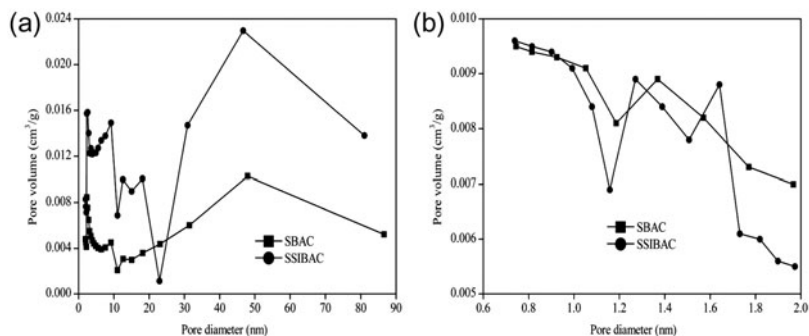


Fig. 7. Pore size distributions of SBAC and SSIBAC: (a) mesopore and (b) micropore size distributions.

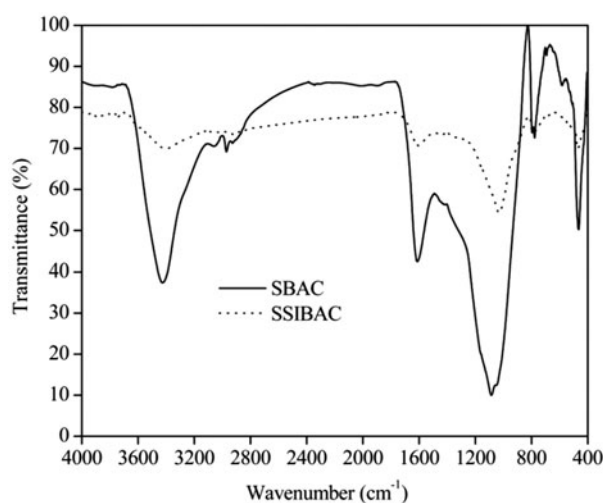


Fig. 8. FTIR spectra of SBAC and SSIBAC.

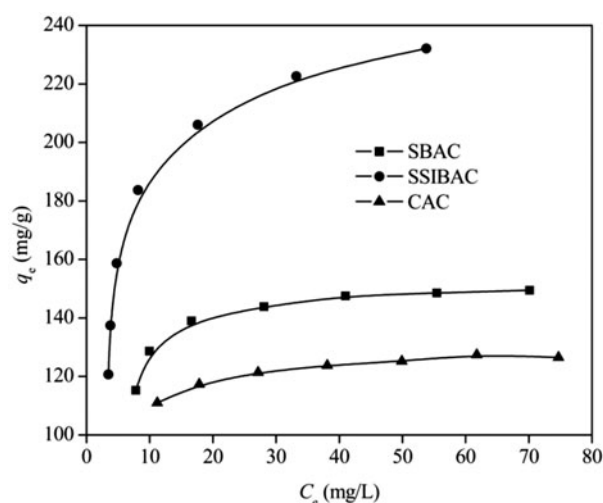


Fig. 9. Adsorption isotherms of AO51 on SBAC, SSIBAC, and CAC.

were carried out as described in section 2.3. For comparison, a commercial activated carbon (CAC) was also studied. The adsorption isotherms of AO51 on SBAC, SSIBAC, and CAC are depicted in Fig. 9. As can be seen, adsorption data of AO51 on the three activated carbons all correspond to isotherm of type I, i.e. convex upward curve, indicative of strong adsorption [32]. Moreover, the addition of scrap iron results in obvious differences in the adsorption performance of the activated carbons for AO51. Two adsorption isotherm models of Langmuir and Freundlich are employed to fit the equilibrium data obtained in the adsorption experiments.

The Langmuir isotherm model assumes that energies of adsorption sites on the surface of adsorbent are homogeneous and monolayer adsorption of adsorbate takes place at specific homogeneous sites. Once an adsorbate molecule occupies a site, no further adsorption can take place at that site. The linear form of Langmuir model is expressed by the following equation [33]:

$$\frac{C_e}{q_e} = \frac{C_e}{q_m} + \frac{1}{K_a q_m} \quad (1)$$

where q_e (mg/g) and C_e (mg/L) are the amount of dye adsorbed by per unit mass of adsorbent and unadsorbed dye concentration in solution at equilibrium, respectively. q_m (mg/g) and K_a (L/mg) are Langmuir constants related to the maximum amount of adsorption and the free energy of adsorption.

The Langmuir isotherm model plots for adsorption of AO51 on SBAC, SSIBAC, and CAC are shown in Fig. 10 and the related parameters are listed in Table 4. The high correlation coefficients ($R^2 > 0.99$ for all activated carbons) suggest that the Langmuir model is suitable for fitting the experimental data.

The essential characteristics of the Langmuir isotherm can be expressed in terms of a dimensionless constant R_L , called separation factor, which is defined as [34]:

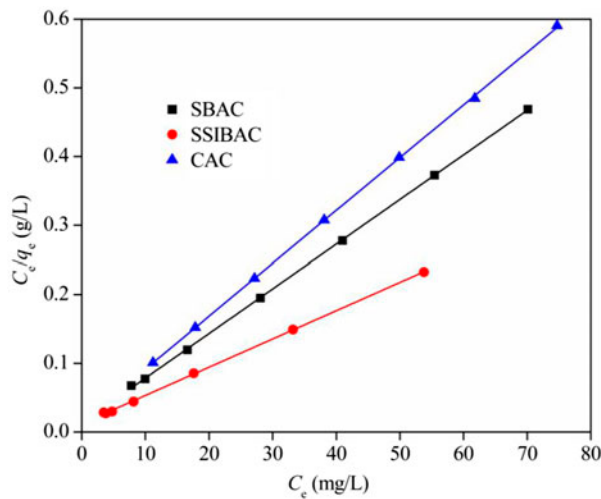


Fig. 10. Langmuir isotherm model plots for adsorption of AO 51 on SBAC, SSIBAC, and CAC.

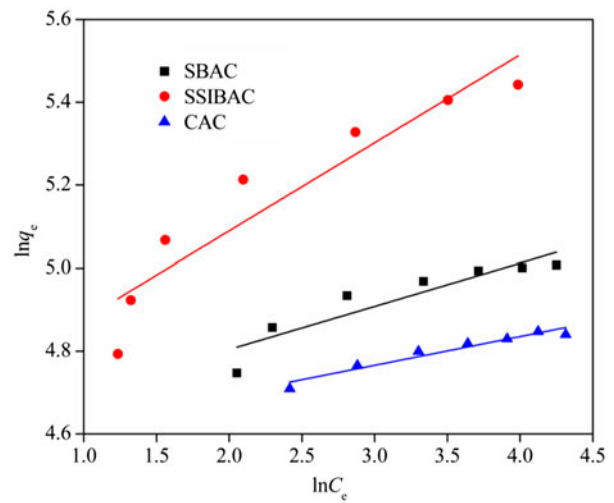


Fig. 11. Freundlich isotherm model plots for adsorption of AO51 on SBAC, SSIBAC, and CAC.

$$R_L = \frac{1}{1 + K_a C_0} \quad (2)$$

where C_0 is the initial dye concentration and K_a is the Langmuir constant. The value of R_L indicates the type of isotherm to be irreversible ($R_L=0$), favorable ($0 < R_L < 1$), linear ($R_L=1$), or unfavorable ($R_L > 1$). In this study, the values of R_L for SBAC, SSIBAC and CAC are 0.021, 0.029 and 0.019, respectively, which are all between 0 and 1, indicating the adsorption of AO51 on SBAC, SSIBAC and CAC is favorable.

The Freundlich model is an empirical equation and assumes that adsorption happens on a heterogeneous surface where energies of adsorption sites are not equivalent, thus allowing multilayer adsorption. The linear form of Freundlich model is represented as [35]:

$$\ln q_e = \ln K_F + \frac{1}{n} \ln C_e \quad (3)$$

where K_F and $1/n$ are Freundlich constants. K_F can roughly indicate the adsorption capacity and $1/n$

gives an indicator of the favorability of adsorption. The $1/n$ values ranging between 0.1 and 1 represent favorable adsorption and bigger values indicate more favorable adsorption.

The Freundlich isotherm model plots for adsorption of AO51 on SBAC, SSIBAC, and CAC are shown in Fig. 11 and the related parameters are listed in Table 4. As shown in Table 4, values of $1/n$ for SBAC, SSIBAC, and CAC all range between 0.1 and 1, indicating the favorable adsorption of AO51 on the activated carbons. In addition, the value of $1/n$ for SSIBAC is bigger than that for SBAC, implying that the adsorption of AO51 is more favorable on SSIBAC than on SBAC.

According to Table 4, compared to the Freundlich model, the correlation coefficients for the Langmuir model are higher, indicating that the Langmuir model describes the adsorption equilibrium of AO51 by SBAC, SSIBAC, and CAC more satisfactorily. Compared to that of SBAC and CAC, the maximum adsorption capacity (q_m) of SSIBAC is the highest, suggesting that SSIBAC performs best in the adsorption of AO51. This phenomenon can be explained as

Table 4
Isotherm parameters of Langmuir and Freundlich models for SBAC, SSIBAC, and CAC

Activated carbon	Langmuir			Freundlich		
	q_m (mg/g)	K_a (L/mg)	R^2	K_F (mg/g)	$1/n$ (L/g)	R^2
SBAC	156.25	0.47	0.999	99.09	0.10	0.817
SSIBAC	243.31	0.34	0.999	106.06	0.21	0.865
CAC	130.38	0.51	0.999	95.33	0.07	0.931

follows. The steric size of AO51 makes the dye molecules susceptible to be confined by the micropores of activated carbons, causing them difficult to get adsorbed in the micropores. Hence, the highly mesoporous structure in SSIBAC results in the highest adsorption capacity for AO51.

4. Conclusion

Activated carbons from sewage sludge with additive scrap iron were prepared using $ZnCl_2$ as activating agent through a traditional pyrolysis process. The experiment results showed that pyrolysis temperature of 550 °C, pyrolysis time of 50 min, impregnation ratio of 3:1, and scrap iron dosage of 0.5 wt % were the optimum preparation conditions. Compared to the sludge-based activated carbon, the sludge with additive scrap iron-based activated carbon had higher specific surface area and larger total pore volume. Adding scrap iron into sewage sludge could remarkably improve the production of mesopores, with the mesopore volume increasing from 0.126 to 0.293 cm^3/g and the mesoporosity increasing from 78 to 89%. Furthermore, the additive scrap iron could enhance the pyrolysis of sludge, thus leading to a slight decrease of some surface functional groups of the activated carbon. In the adsorption experiments, the addition of scrap iron improved the performance of the activated carbon in the adsorption of an anionic azo dye. The Langmuir model described the adsorption equilibrium of the dye by the activated carbons satisfactorily. The maximum adsorption capacity of the activated carbon for the dye was significantly increased after the addition of scrap iron due to the formation of more mesopores.

Acknowledgment

The work was financially supported by National Natural Science Foundation of China (No. 51008106).

References

- [1] N. Litz, Assessment of organic constituents in sewage sludge, *Water Sci. Technol.* 42 (2000) 187–193.
- [2] G. Mininni, C.M. Braguglia, D. Marani, Partitioning of Cr, Cu, Pb and Zn in sewage sludge incineration by rotary kiln and fluidized bed furnaces, *Water Sci. Technol.* 41 (2000) 61–68.
- [3] P.C. Chiang, J.H. You, Use of sewage sludge for manufacturing adsorbents, *Can. J. Chem. Eng.* 65 (1987) 922–927.
- [4] A. Méndez, G. Gascó, M.M.A. Freitas, G. Siebielec, T. Stuczynski, J.L. Figueiredo, Preparation of carbon-based adsorbents from pyrolysis and air activation of sewage sludges, *Chem. Eng. J.* 108 (2005) 169–177.
- [5] L.F. Calvo, M. Otero, A. Morán, A.I. García, Upgrading sewage sludges for adsorbent preparation by different treatments, *Bioresour. Technol.* 80 (2001) 143–148.
- [6] X. Fan, X. Zhang, Adsorption properties of activated carbon from sewage sludge to alkaline-black, *Mater. Lett.* 62 (2008) 1704–1706.
- [7] T.H. Kim, Y.K. Nam, C. Park, M. Lee, Carbon source recovery from waste activated sludge by alkaline hydrolysis and gamma-ray irradiation for biological denitrification, *Bioresour. Technol.* 100 (2009) 5694–5699.
- [8] J.H. Tay, X.G. Chen, S. Jeyaseelan, N. Graham, Optimising the preparation of activated carbon from digested sewage sludge and coconut husk, *Chemosphere* 44 (2001) 45–51.
- [9] C. Wu, M. Song, B. Jin, Y. Wu, Y. Huang, Effect of biomass addition on the surface and adsorption characterization of carbon-based adsorbents from sewage sludge, *J. Environ. Sci.* 25 (2013) 405–412.
- [10] M. Sereych, T.J. Bandosz, Removal of cationic and ionic dyes on industrial–municipal sludge based composite adsorbents, *Ind. Eng. Chem. Res.* 46 (2007) 1786–1793.
- [11] M. Gheju, A. Iovi, Kinetics of hexavalent chromium reduction by scrap iron, *J. Hazard. Mater.* 135 (2006) 66–73.
- [12] X. Dong, W. Ding, X. Zhang, X. Liang, Mechanism and kinetics model of degradation of synthetic dyes by UV-vis/ H_2O_2 /ferrioxalate complexes, *Dyes Pigm.* 74 (2007) 470–476.
- [13] A. López-López, J.S. Pic, H. Debellefontaine, Ozonation of azo dye in a semi-batch reactor: A determination of the molecular and radical contributions, *Chemosphere* 66 (2007) 2120–2126.
- [14] Y. Liu, X. Chen, J. Li, C. Burda, Photocatalytic degradation of azo dyes by nitrogen-doped TiO_2 nanocatalysts, *Chemosphere* 61 (2005) 11–18.
- [15] M.D.G. De Luna, E.D. Flores, D.A.D. Genuino, C.M. Futral, M.W. Wan, Adsorption of Eriochrome Black T (EBT) dye using activated carbon prepared from waste rice hulls—Optimization, isotherm and kinetic studies, *J. Taiwan Inst. Chem. Eng.* 44 (2013) 646–653.
- [16] Y.S. Al-Degs, M.A.M. Khraisheh, S.J. Allen, M.N. Ahmad, Adsorption characteristics of reactive dyes in columns of activated carbon, *J. Hazard. Mater.* 165 (2009) 944–949.
- [17] N. Sato, An overview on the passivity of metals, *Corros. Sci.* 31 (1990) 1–19.
- [18] M.S. Odziemkowski, R.P. Simpraga, Distribution of oxides on iron materials used for remediation of organic groundwater contaminants—Implications for hydrogen evolution reactions, *Can. J. Chem.* 82 (2004) 1495–1506.
- [19] American Standard of Testing Material. Standard test method for determination of iodine number of activated carbon, Annual Book of ASTM standards, D4607-94, Philadelphia, 1986, pp. 542–545.
- [20] Japanese Standard Association, Standard testing method of methylene blue number of activated carbon, Japanese industrial standard test method for activated carbon, JIS K 1470–1991, Tokyo, 1992.
- [21] D.M. Schnur, M.V. Grieshaber, J.P. Bowen, Development of an internal searching algorithm for parameterization of the MM2/MM3 force fields, *J. Comput. Chem.* 12 (1991) 844–849.

- [22] K. Sun, J.C. Jiang, Preparation and characterization of activated carbon from rubber-seed shell by physical activation with steam, *Biomass Bioenergy* 34 (2010) 539–544.
- [23] A. Linares-Solano, I. Martín-Gullón, C. Salinas-Martínez de Lecea, B. Serrano-Talavera, Activated carbons from bituminous coal: Effect of mineral matter content, *Fuel* 79 (2000) 635–643.
- [24] C. Liu, Z. Tang, Y. Chen, S. Su, W. Jiang, Characterization of mesoporous activated carbons prepared by pyrolysis of sewage sludge with pyrolusite, *Biomass Bioenergy* 101 (2010) 1097–1101.
- [25] H. Marsh, B. Rand, The process of activation of carbons by gasification with CO₂-II. The role of catalytic impurities, *Carbon* 9 (1971) 63–77.
- [26] A. Tomita, K. Higashiyama, Y. Tamai, Scanning electron microscopic study on the catalytic gasification of coal, *Fuel* 60 (1981) 103–114.
- [27] H. Marsh, M.A. Diez, K. Kuo, In: J. Lahaye, P. Ehrburger, *Fundamental Issues in Control of Carbon Gasification Reactivity*, Kluwer Academic, Dordrecht, vol. 205, 1991.
- [28] A. Oya, S. Yoshida, J. Alcaniz-Monge, A. Linares-Solano, Formation of mesopores in phenolic resin-derived carbon fiber by catalytic activation using cobalt, *Carbon* 33 (1995) 1085–1090.
- [29] V. Zubkova, V. Prezhdo, P. Borowiec, A. Ryncarz, The influence of mineral matter on transport of coal plastic mass and on volume of coal charge during carbonisation, *Fuel Process. Technol.* 86 (2005) 1403–1417.
- [30] O. Duggan, S.J. Allen, Study of the physical and chemical characteristics of a range of chemically treated, lignite based carbons, *Water Sci. Technol.* 35 (1997) 21–27.
- [31] C. Jindarom, V. Meeyoo, B. Kitiyanan, T. Rirksomboon, P. Rangsunvigit, Surface characterization and dye adsorptive capacities of char obtained from pyrolysis/gasification of sewage sludge, *Biochem. Eng. J.* 133 (2007) 239–246.
- [32] S. Brunauer, P. Emmett, E. Teller, Adsorption of gases in multimolecular layers, *J. Am. Chem. Soc.* 60 (1938) 309–319.
- [33] I. Langmuir, The adsorption of gases on plane surfaces of glass, mica and platinum, *J. Am. Chem. Soc.* 40 (1918) 1361.
- [34] K.R. Hall, L.C. Eagleton, A. Acrivos, T. Vermeulen, Pore- and solid-diffusion kinetics in fixed-bed adsorption under constant-pattern conditions, *Ind. Eng. Chem. Fundam.* 5 (1966) 212–223.
- [35] H. Freundlich, Adsorption in solution, *Phys. Chem. Soc.* 40 (1906) 1361–1368.